

Naringenin prevents high glucose-induced mitochondria-mediated apoptosis involving AIF, Endo-G and caspases

Radhika Kapoor · Fatima Rizvi · Poonam Kakkar

Published online: 29 November 2012
© Springer Science+Business Media New York 2012

Abstract Oxidative stress is implicated in hyperglycemia-induced alterations in cell signaling pathways. We examined the toxicity of high glucose in primary rat hepatocytes and its amelioration by naringenin. Incubation of hepatocytes with 40 mM glucose for 1.5 h exhibited significant decrease in cell viability confirmed by MTT reduction and Alamar blue assay. At the same time primary rat hepatocytes exhibited significant decrease in mitochondrial membrane potential indicating organelle dysfunction. Enhanced translocation of Cyt-c from mitochondria to cytosol and AIF/Endo-G from mitochondria to nucleus, activation of caspase-9/3, DNA damage, and chromatin condensation were observed in glucose-stressed hepatocytes, indicating the involvement of mitochondrial pathway in high glucose-induced apoptosis. Transcript levels of antioxidant enzymes were significantly altered along with corresponding changes in their enzymatic activities. The level of intracellular antioxidant glutathione as well as superoxide dismutase, catalase, and glutathione peroxidase activities were observed to be significantly decreased in hepatocytes treated with high concentration of glucose. Naringenin, a flavanone, was effective in preventing loss of cell viability, reactive oxygen species generation, and decline in antioxidant defense. Translocation of AIF, Endo-G, and Cyt-c from mitochondria was also inhibited by naringenin in glucose-stressed cells. Messenger RNA expression of anti-apoptotic and apoptotic genes, externalization of phosphatidyl serine, DNA damage, chromatin condensation, and sub-diploid cell population were effectively altered by naringenin indicating its anti-apoptotic potential in vitro. Our data suggests that naringenin can

prevent apoptosis induced by high glucose through scavenging of reactive oxygen species and modulation of mitochondria-mediated apoptotic pathway.

Keywords Glucose toxicity · Apoptosis · Oxidative stress · Mitochondrial dysfunction · Apoptosis inducing factor · Naringenin

Abbreviations

$\Psi\Delta m$	Mitochondrial membrane potential
AGE	Advanced glycated end products
AIF	Apoptosis inducing factor
Bax	Bcl-2 associated X
Bcl-2	B-cell lymphoma-2
CAT	Catalase
cDNA	Complementary DNA
COX-II	Cyclo-oxygenase-II
CuZn-SOD	Copper-zinc superoxide dismutase
Cyt-c	Cytochrome c
DCF	Dichlorofluorescein
DCFH-DA	2',7'-Dichlorofluorescein diacetate
EDTA	Ethylenediaminetetraacetic acid
Endo-G	Endonuclease-G
FITC	Fluorescein isothiocyanate
GAPDH	Glyceraldehyde 3 phosphate dehydrogenase
GR	Glutathione reductase
GPx	Glutathione peroxidase
GSH	Reduced glutathione
HRP	Horseradish peroxidase
JC-1	5,5',6,6'-Tetrachloro-1,1',3,3'-tetraethylbenzimidazol-carbocyanine iodide
MnSOD	Manganese superoxide dismutase
MPT	Mitochondrial permeability transition
MTT	3-(4,5-dimethylthiazol-2-yl)-2, 5-diphenyl tetrazolium bromide

R. Kapoor · F. Rizvi · P. Kakkar (✉)
Herbal Research Section, CSIR-Indian Institute of Toxicology
Research, P.O. Box-80, M.G.Marg, Lucknow 226001, India
e-mail: poonam_kakkar@yahoo.com

NAFLD	Non-alcoholic fatty liver disease
NBT	Nitroblue tetrazolium
<i>p</i> -NA	<i>p</i> -nitro aniline
PBS	Phosphate buffered saline
PKC	Protein kinase c
PVDF	Polyvinylidene fluoride
ROS	Reactive oxygen species
RT-PCR	Reverse transcriptase polymerase chain reaction
SOD	Superoxide dismutase

Introduction

Diabetes mellitus entails several chronic metabolic disorders characterized by hyperglycemia and absolute or relative insulin deficiency. Its incidence is increasing both in industrialized as well as developing countries. According to WHO, 552 million people in the world will have diabetes by the year 2030 [1]. Long-term hyperglycemia leads to a high concentration of glucose in the circulation, leading to functional and structural deficits in the cells. Diabetes pandemic is a major cause of morbidity and mortality worldwide, which has an impact on the overall cost for public health. Importance of early implementation of preventive and therapeutic strategies is an undebatable issue in the management of hyperglycemia [2].

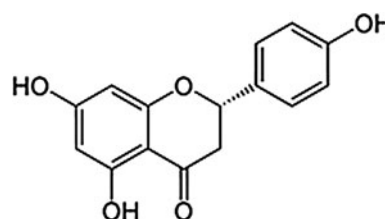
Increased oxidative stress and depleted antioxidant defenses are considered to be critical in progression of diabetes. Oxidative stress in the cell occurs due to increased production of reactive oxygen species (ROS) and decreased levels of antioxidants [3]. In mitochondria, increased ROS production reportedly results from hyperglycemia-induced increase in the proton gradient across the inner mitochondrial membrane. Proton gradient beyond a threshold value causes blocked complex III electron transfer, release of electrons from ubiquinone and finally leads to the formation of superoxide [4]. Four major mechanisms are proposed for hyperglycemia-induced ROS associated tissue damage: (i) the polyol pathway, (ii) the hexosamine pathway, (iii) protein kinase C (PKC) activation, and (iv) formation of advanced glycated end-products (AGE) [4].

High concentration of glucose generates ROS which often plays a major role in glucose-induced cellular dysfunction and appears to underlie the development of various diabetic complications [2, 3]. This condition in addition to inducing various metabolic dysfunctions contributes to progressive development of micro- and macro vascular complications and multi-organ damage. Recent scientific reports indicate that oxidative stress is the biochemical trigger for hepatic dysfunction in diabetic rats [5, 6]. In the absence of an appropriate counteracting response from the intrinsic

antioxidant network against glucotoxicity caused by hyperglycemia, oxidative stress becomes predominant, leading to activation of the stress-sensitive intracellular signaling pathway. However, little is known about the direct toxic effects of high glucose concentration on hepatic cells. Disruption of cellular signal transduction pathways, especially the apoptosis signaling pathways could be one of the possible mechanisms for hyperglycemia-induced cell death.

The conventional death of a cell undergoing apoptosis includes translocation of various apoptotic proteins from their resident places, DNA fragmentation, nuclear condensation, cell shrinkage, blebbing, and externalization of phosphatidylserine [7, 8]. These events are concerted and co-ordinated by the activity of a family of cysteine proteases called caspases [9]. Apoptotic stress causes mitochondrial outer membrane permeabilization, and hence mitochondrial dysfunction. This process is controlled by the pro- and anti-apoptotic members of the Bcl-2 family and leads to the cytosolic release of mitochondrial inter-membrane space proteins that can trigger either caspase-activated or caspase-independent death pathways [10, 11]. Certain caspase-independent death effectors in mitochondria have also been reported, to name a few—apoptosis inducing factor (AIF) and endonuclease G (Endo-G) [12]. During apoptosis, Endo-G and AIF translocate to the nucleus where they cause oligonucleosomal DNA fragmentation [13]. Apoptosis inducing factor in its mature state is located in the inner mitochondrial membrane and is of 62 kDa. Whenever there is an apoptotic stimuli, AIF is cleaved to smaller size of an approximately 57 kDa form in the mitochondrial inter-membrane space; from here it gets released into the cytoplasm and translocated into the nucleus where it intervenes apoptosis by causing chromatin condensation and DNA fragmentation.

Many herbal medicines have been recommended as single agents or in different oral formulations for management of diabetes mellitus due to the fact that they are less toxic and more effective in controlling glucose release from liver than oral hypoglycemic agents such as sulfonylurea, metformin etc. [14, 15]. Grapefruit, *Citrus paradisi* is traditionally known to have medicinal importance. This plant has various bio-active compounds which can be used efficiently in the prevention of toxicity. Naringenin, a flavanone present in this plant, is considered to have beneficial effects on human health as anti-inflammatory, carbohydrate metabolism promoter, and immune system modulator [16].



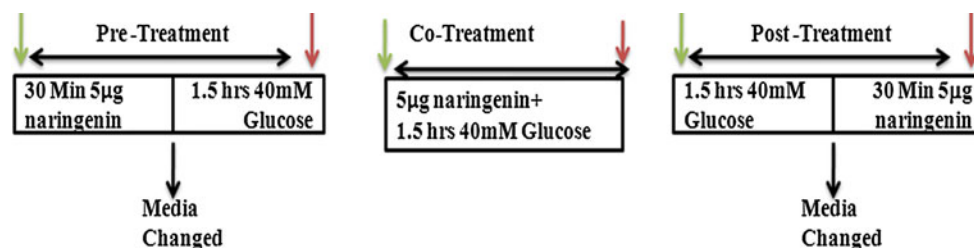
In the present study we have made an attempt to investigate the mechanism of cell death in primary rat hepatocytes upon exposure to high concentration of glucose in which alterations in endogenous antioxidative systems and regulation of stress-sensitive signaling pathways have been studied. Capacity of naringenin to provide protection against hyperglycemia-induced changes in mitochondria-mediated apoptotic pathway in primary rat hepatocytes has been studied in depth along with its capacity to counter oxidative stress.

Materials and methods

Animals

Animal handling in all experimental procedures was approved by the Institutional Animal Ethics Committee (ITRC/IAEC/20/2010). Male Wistar rats weighing 180 ± 20 g from Indian Institute of Toxicology Research (IITR) animal colony were used for the experiments. Rats were housed in an air conditioned room at 25 ± 2 °C temperature with 60–70 % humidity and a controlled 12 h

(Thermo-forma) with controlled humidity at 37 °C. The cells were seeded at a density of 1.0×10^4 cells/well in 0.1 % collagen pre-coated 96-well plates, and used for experiments after being cultured for 24 h. Three different treatment regimes were used. In pre treatment, 5 μ g naringenin per 10,000 cells was given to the cells for 30 min, change of media followed by 1.5 h exposure to high glucose (40 mM). In co-treatment, cells were exposed to naringenin and high glucose simultaneously for 1.5 h. In post treatment after the high glucose exposure for 1.5 h, media was changed and naringenin was added for 30 min. Descriptive illustration of same is given below. Cells were harvested just after the end of time period of respective treatments. Cells were cultured with high concentrations of glucose to mimic the hyperglycemic condition [10, 11, 13]. Forty millimolar glucose has been explicitly used to depict hyperglycemic condition by many researchers [18–20]. In addition to it, 40 mM glucose concentration has been reported in neonates and adult diabetic patients [21–23]. Leininger et al. [19] have reported that high glucose can induce apoptosis within 30 min exposure time. To exclude a hyper-osmolar effect, identical concentration of mannitol was added in control cells.



light/dark cycle. Rats were fed on standard pellet diet (Ashirwad Pellet Diet, Mumbai, India) and water ad libitum. Chloroform was used for euthanasia. Rats were fasted overnight before preparation of primary hepatocytes.

Cell culture

Primary hepatocytes were isolated from liver of overnight fasted Wistar rat according to the two step collagenase perfusion method [17]. Cell viability was checked by trypan blue dye exclusion test within 1 h of cell isolation. Only preparations with cell viability greater than 95 % were used for subsequent experiments. Hepatocytes were maintained in RPMI-1640 media supplemented with heat-inactivated 10 % fetal bovine serum and 1 % of 10,000 units Penicillin, 10 mg Streptomycin, 25 μ g Amphotericin B, 1 mM sodium pyruvate, 2 mM glutamine under an atmosphere of 5 % CO₂–95 % air in an incubator

Quantitative analysis of viable cells

MTT reduction assay

Mitochondrial metabolic activity in hepatocytes, following the treatment schedule, was determined by MTT assay [24]. This is a colorimetric assay that measures the reduction of yellow 3-(4,5-dimethylthiazol-2-yl)-2,5-diphenyl tetrazolium bromide (MTT) by mitochondrial succinate dehydrogenase. 3-(4, 5-Dimethylthiazol-2-yl)-2,5-diphenyl tetrazolium bromide enters the cells and passes into the mitochondria where it is reduced to an insoluble, coloured (dark purple) formazan product. The cells are then solubilised with an organic solvent and the released, solubilised formazan reagent is measured spectrophotometrically at 530 nm. The data is expressed as percentage of viability compared to control cells.

Cell viability assay by Alamar blue

The active ingredient of Alamar blue (resazurin) is a non-toxic, cell permeable compound that is blue in color and virtually non-fluorescent. Upon entering cells, resazurin is reduced to resorufin which is a highly fluorescent red compound. Viable cells convert resazurin to resorufin, thereby generating a quantitative measure of viability. Alamar blue assay was done according to manufacturer's protocol (Invitrogen, Carlsbad, CA). Fluorescence intensity was measured on a spectrofluorimeter (Varioskan Flash, Thermo) at excitation and emission wavelengths of 530 and 570 nm, respectively.

Antioxidant status of treated hepatocytes

Superoxide dismutase activity

Superoxide dismutase assay is based on the spectrophotometric assessment of the inhibition of nitro blue tetrazolium-NADH and phenazine methosulphate (PMS)-mediated formazan formation. Superoxide dismutase activity was done according to the method of Kakkar and Vishwanathan [25]. Absorbance was measured at 560 nm. Fifty percentage of inhibition of formazan formation under the assay conditions in 1 min is taken as one unit of enzyme activity/minute.

Catalase activity

Catalase was assayed spectrophotometrically using the method by Aebi [26]. Catalase activity is expressed as $\mu\text{M H}_2\text{O}_2$ decomposed/min/ 10^4 cells. Assay is based on the principle of determining decomposition of H_2O_2 by catalase which is measured at 240 nm.

Reduced glutathione (GSH)

Reduced glutathione was measured using the method described by Dringen and Hamprecht [27] with some modifications. Fifty microliters of cell lysate was diluted with 50 μl of 100 mM phosphate buffer containing 1 mM EDTA. To this mixture 100 μl of reaction buffer [295 μM 5,5'-dithio-bis (2-nitrobenzoic acid) (DTNB) made in 10 ml of phosphate buffer] was added and measured at 412 nm within 5 min. Reduced glutathione from Sigma was employed to obtain a standard curve. Reduced glutathione is expressed as $\mu\text{M GSH}/10^4$ cells.

Glutathione peroxidase

Glutathione peroxidase activity was measured by using the method of Paglia and Valentine [28]. Reaction mixture

contained 2.525 ml of 0.1 M Tris HCl buffer (pH 7.2), 75 μl of 0.04 M GSH, 100 μl of 0.1 M nicotinamide adenine dinucleotide phosphate (NADPH) and 100 μl of glutathione reductase (0.24 units). Fifteen to twenty microliters of cell lysate was added to the reaction mixture. Reaction was initiated by adding 100 μl of 0.75 mM hydrogen peroxide. The decrease in absorbance was measured at 340 nm for 3 min at every 30 s. The activity was expressed as nM NADPH oxidized/mg protein/min using molar extinction coefficient of $6.22 \times 10^3/(\text{mM}/\text{cm})$.

Measurement of ROS production in the cells

Reactive oxygen species generation in hepatocytes was measured by method of Zhang et al. [29] using the cell permeable fluorescent dye 2',7'-dichlorofluoresceindiacetate (DCFH-DA). Upon entering the cell, the diacetate bond of the fluoroprobe is cleaved by intracellular esterases leaving DCFH which is oxidized to DCF by the oxidants and its fluorescence is taken as an indicator of ROS production in the cell. The fluorescence intensity was measured on a spectrofluorimeter (Varioskan Flash, Thermo) at excitation and emission wavelengths of 485 and 530 nm, respectively.

Expression of antioxidant, apoptotic and antiapoptotic genes

Total RNA was isolated from treated and untreated hepatocytes by using the Trizol reagent (Invitrogen, Carlsbad, CA, USA) according to the manufacturer's instructions. Three micrograms of total RNA was reverse transcribed (RT) into cDNA using Revert Aid H minus First Strand cDNA Synthesis Kit (Fermentas, EU) as per manufacturer's instructions. After reverse transcription, cDNA was used for semi-quantitative PCR using sets of specific primers as shown in Table 1. cDNA amplification was carried out according to the respective temperature profile and number of cycles for Bax, Bcl-2, Caspase-3, Caspase-9, GPx, GR, Mn-SOD, and CuZn-SOD. Glyceraldehyde 3 phosphate dehydrogenase was used as internal control. Five microliters of the product was run on 1.5 % agarose gel, and photographed on UV transilluminator (Alfa-Innotech; CellBio- 264 sciences Inc., SantaClara, CA) using a digital camera. Polymerase chain reaction products were analyzed using Image J software 1.44 (USA) and normalized to GAPDH.

Mitochondrial membrane potential

Loss of the mitochondrial membrane potential can be measured using fluoroprobe JC-1. In cells with low membrane potential (depolarized mitochondria), JC-1 is in its

Table 1 Primers used for expression of apoptotic, anti-apoptotic and antioxidant genes

Genes	Primers
Bcl-2	F 5'-ACTTTGCAGAGATGTCCAGTCAG-3' R 5'-GTTTCAGGTAAGTCCAGTCATCCACAG-3'
Bax	F 5'-GGAGGAAGTCCAGTGTCCAG-3' R 5'-TGCAGAGGATGATTGCTGAC-3'
GPx	F 5'-CAGTTCGGACATCAGGAGAAT-3' R 5'-AGAGCGGGTGAGCCTTCT-3'
GR	F 5'-GGGCAAAGAAAGATTCCAGGTT-3' R 5'-GGAGGCTTCATCTTCAGTGA-3'
MnSOD	F 5'-CGTGCTCCCACACATCAATC-3' R 5'-TGAACGTCACCGAGGAGAAG-3'
CuZn-SOD	F 5'-CGTCATTCATCTCGAGCAGA-3' R 5'-CACCTTTGCCAAAGTCATCT-3'
Caspase-3	F 5'-GAACGAACGGACCTGTGGACCT-3' R 5'-GCCTCCACTGGTATCTTCTGGCAT-3'
Caspase-9	F 5'-TGAGCCAGATGCTGTCCCATACCAG-3' R 5'-CCTGGGAAGGTGGAGTAGGACAC-3'
GAPDH	F 5'-GGCCAAGATCATCCATGACAACT-3' R 5'-ACCAGGACATGAGCTTGACAAAGT-3'

monomeric form, which has green fluorescence. In cells with high membrane potential (polarized mitochondria), formation of dimers of the dye is promoted, resulting in red fluorescence. A decrease in red/green ratio indicates an increase in depolarized mitochondria. Cultured cells were incubated with 2.5 $\mu\text{g/ml}$ of JC-1 fluoroprobe at 37 °C in dark for 30 min. After washing the hepatocytes, $\Delta\Psi\text{m}$ was assessed by comparing two fluorescence, i.e. red (Ex/Em-580/590 nm)/green (Ex/Em-510/527 nm) using Varioskan fluorescent microplate reader [30].

Preparation of sub-cellular fractions

From control and treated primary rat hepatocytes, nuclear fractions were obtained as described by Leal et al. [11] whereas cytosolic and mitochondrial fractions were prepared as described by Tripathi et al. [30].

Immunoblot analysis

The protein content corresponding to each treatment was quantified by method described by Lowry et al. [31]. Samples were incubated with loading dye for 5 min at 96 °C and immediately kept on ice. Sixty microgram of protein sample from nuclear, cytosolic or mitochondrial fraction was separated by electrophoresis on 12 % SDS-polyacrylamide gel and electro blotted on PVDF membrane (HybondTM -P

Amersham Biosciences, UK limited, NA). After blocking non-specific sites with 1 \times blocking buffer (Sigma), washing was performed using TBS containing 0.1 % Tween-20 (TBS-T). The membrane was then incubated for 1 h with specific polyclonal IgG antibodies of Cyt-c, Bax, Bcl-2, caspase-3, caspase-9, AIF, Endo-G, Cox IV, Lamin B, and β -Actin (Santa Cruz Biotechnology, Inc.) in 1:500 dilutions. This was followed by washing with TBS-T and incubation with horse-radish peroxidase-conjugated rabbit anti-goat IgG, goat anti-rabbit IgG or goat anti-mouse IgG secondary antibodies in 1:1000 dilutions for 1 h at room temperature. Membrane was rewashed and the immunoblot was revealed using ImmobilonTM Western Chemiluminescent HRP substrate kit. (Millipore, Corporation, MA, USA). PageRulerTM Prestained Protein Ladder (5 μl of SM-0671 from Fermentas, EU) was used to determine molecular weight of the protein bands. Densitometry of the bands obtained was done using NIH software Image J version 1.41 (USA). Band areas were calculated by densitometric scanning and result expressed as Arbitrary Units for each experimental band. Experiment was repeated more than three times and similar results were obtained.

Immunocytochemical detection of translocation of AIF

Prior to the treatment schedule, cells were treated with 1 μM Mitotracker Orange dye (Invitrogen) for 30 min. After treatment, cells were fixed with a solution of 4 % paraformaldehyde for 10 min at room temperature, followed by rinsing twice in PBS and permeabilization with 1 % Triton X-100 in PBS for 5 min. After blocking for 30 min with 10 % rabbit serum in PBS with 0.2 % Tween-20, cells were incubated with the primary antibody anti-AIF (1:100) for 90 min. Cells were rinsed three times with PBS and incubated with FITC-conjugated secondary antibody (rabbit anti-goat IgG, 1:500). Nuclei were stained with Hoechst 33258 stain for 10 min. The preparations were visualized with an upright fluorescent microscope (Leica DMRB Fluorescence Microscope, Wetzlar, Germany). Images were captured under 63 \times objective.

Caspase-3 enzymatic activity

The proteolytic reaction was conducted in isolation buffer containing 10 mM Tris-HCl buffer, pH 7.6, 5 mM MgCl_2 , 1.5 mM potassium acetate, 2 mM DTT, and protease inhibitor. Reaction mixture consisted of 50 μg of cytosolic protein and 50 μM Asp-Glu-Val-Asp-pNA in isolation buffer. General caspase activity was evaluated by enzymatic cleavage of chromophore *p*-nitroanilide (pNA) from the substrate *N*-acetyl-Asp-Glu-Val-Asp-pNA (Sigma). The reaction mixtures were incubated at 37 °C for 1 h, and

the formation of pNA was measured at 405 nm using Varioskan flash plate reader [32].

DNA fragmentation

DNA was isolated from control and treated hepatocytes [30] and DNA quantification was done spectrophotometrically at 260/280 nm on NanoDrop spectrophotometer Q20 (ND-1000; NanoDrop Technologies, Inc., USA). DNA samples were finally separated by electrophoresis on 1.8 % agarose gel with Tris–Borate/EDTA buffer and analyzed on Alfa-Innotech (CellBio- 264 sciences Inc., SantaClara, CA) image analyzer.

Fluorographic monitoring of apoptosis-associated nuclear alterations

Changes in the nuclear morphology were observed using bisbenzimidazole (Hoechst 33258) fluorochrome that binds specifically to ATAT rich regions of DNA. Primary hepatocyte monolayer (treated and control) were fixed in 4 % paraformaldehyde for 10 min. Cells were then stained with Hoechst 33258 (5 µg/ml) for 10 min followed by washing and mounting in a solution of 20 mM citric acid, 50 mM disodium orthophosphate, and 50 % glycerol (pH 5.5). Apoptosis-associated nuclear alterations were examined at a wavelength of Ex/Em-350/460 nm using Nikon microscope (TS 80i, Leica, Wetzlar, Germany) with fluorescence attachment [30].

Annexin V binding assay

The externalization of phosphatidylserine on cell membrane surface was detected by FITC tagged annexin V stain using Annexin V-FITC Apoptosis detection kit (APOAF; Sigma, St. Louis, MO, USA). Briefly, hepatocytes were aliquoted and to this Annexin V fluorescein isothiocyanate (FITC) was mixed. Cells were incubated for 15 min and PI was added to distinguish the necrotic cells based on following characteristics. (a) Viable hepatocytes are negative for both Annexin V and PI, (b) Early apoptotic hepatocytes were labeled with Annexin V while were negative for PI, (c) Late apoptotic cells were labeled with both Annexin V and PI, (d) Necrotic cells take up only PI. Acquisition of stained cells was done on flow cytometer (BD-LSR) and analysis performed using Cell Quest software. Each determination is based on acquisition of 10,000 events [30].

Apoptotic DNA content

To determine the population of apoptotic cells, analysis was done using propidium iodide (PI) staining.

Hepatocytes were collected and centrifuged at 800 g for 5 min, washed once with cold PBS and fixed in 70 % chilled ethanol. Fixative was decanted and to the fixed cells 0.1 % Triton X-100 was added. Cells were again washed with PBS and resuspended in PBS containing 50 µg/ml PI and 1 mg/ml RNase A for 30 min in the dark at 4 °C. Labeled nuclei were subjected to flow cytometric analysis and then gated on light scatter to remove debris. The percentage of nuclei with sub-G1 content was considered apoptotic cells. Propidium Iodide fluorescence was measured through a FL-2 filter (585 nm) [33].

Statistical analysis

Data are expressed as mean ± SE. Data was analyzed on SPSS software version 14.0 using one-way ANOVA. $P < 0.05$ was used as the criterion for significance.

Results

High glucose-induced cytotoxicity and oxidative stress in primary rat hepatocytes

High glucose decreased hepatocyte survival significantly

In order to evaluate the cytotoxic potential of glucose, hepatocytes were treated with varying concentrations of glucose (10–40 mM) and their viability measured by MTT assay and Alamar blue assay as shown in Fig. 1a. To exclude a hyper-osmolar effect, identical concentration of mannitol was added to control cells. At 40 mM glucose concentration, the cell survival decreased by 49.89 % ($P < 0.05$) as assessed by MTT and 46.78 % as assessed by Alamar blue assay. However, no change was observed in viability of cells treated with equal concentration (40 mM) of mannitol which excludes the possibility of hyper-osmolar effect.

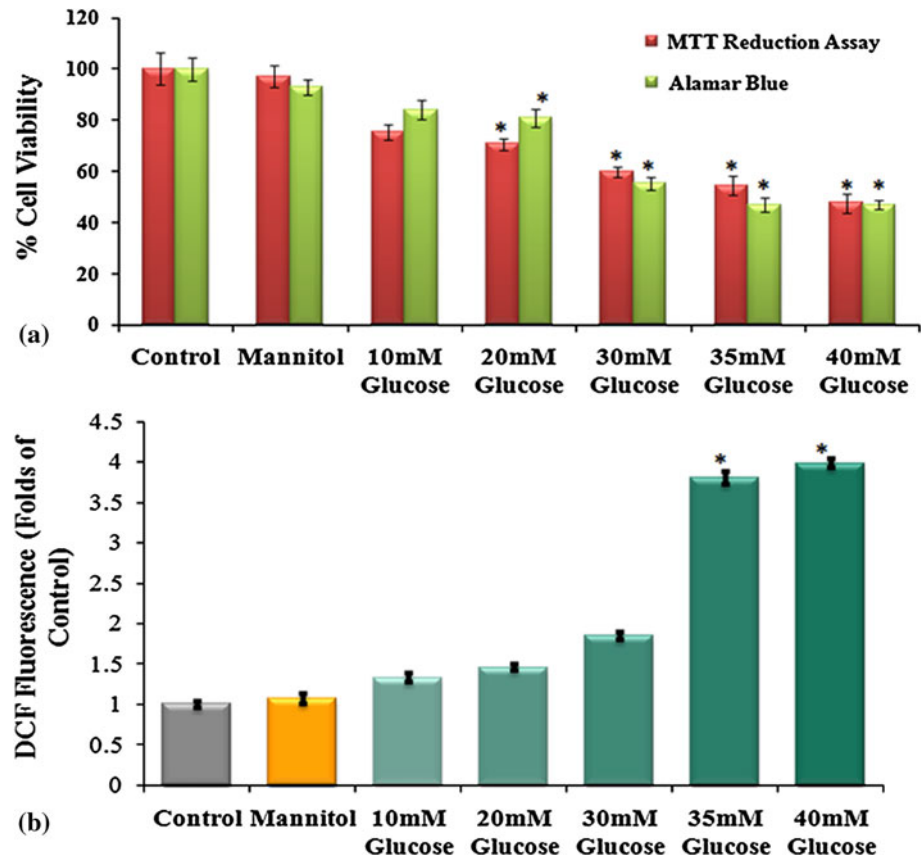
Glucose stress increased intracellular ROS generation

There was 3.98-fold ($P < 0.05$) increase in intracellular ROS generation in 40 mM glucose-stressed hepatocytes as assessed by DCFH-DA fluoroprobe whereas 40 mM mannitol treated cells did not show any significant increase in intracellular ROS generation and was comparable to control (Fig. 1b). The data confirms that high glucose stress (40 mM) causes significant ROS generation.

Effect of high glucose stress on antioxidant status

In control hepatocytes, the SOD activity was found to be 0.82 ± 0.01 U/min/ 1×10^4 cells. Cultured hepatocytes

Fig. 1 Cell viability and ROS generation in the presence of varying concentrations of glucose. Effect of increasing concentration of glucose on viability of primary hepatocytes. **a** Cell viability as assessed by MTT and Alamar blue assay and **b** ROS generation as fold of DCF fluorescence as compared to control in cells exposed to increasing concentration of glucose. Results are shown as mean \pm SE from three independent experiments. Significant difference compared with control values * $P < 0.05$, $n = 6$



when treated with increasing concentration of glucose (10–40 mM) showed a gradual decrease in SOD activity which was $0.27 \text{ U/min}/1 \times 10^4 \text{ cells}$ ($P < 0.05$), in the presence of 40 mM glucose (Table 2). However, SOD activity in mannitol treated cells was almost equal to that of control cells. As evident from Table 2, catalase activity was significantly reduced by 46.92 % ($P < 0.05$) in 40 mM glucose-treated cells. Intracellular reduced glutathione (GSH) content exhibited a 2.6-fold decrease ($P < 0.05$) in 40 mM glucose-treated cells.

Effect of Naringenin on glucose-induced apoptosis in primary hepatocytes

Naringenin protects against high glucose-induced cytotoxicity

Cell viability of hepatocytes treated with selected dose (40 mM) of glucose and naringenin (5 μg) under different treatment regime (pre/co/post-treatment) showed increase by 30 % ($P < 0.05$), 49 % ($P < 0.05$), 26 % ($P < 0.05$) in pre exposure, co-exposure and post-exposure respectively, when compared to glucose-treated cells (Fig. 2a), while there was no significant change observed in hepatocytes treated with only naringenin.

Prevention of ROS generation by naringenin

Intracellular ROS generation under different exposure conditions (pre, co and post) was estimated using DCFH-DA fluoro-probe. Cells co-treated with naringenin showed a highly significant ($P < 0.05$) decline in the ROS generation i.e. 51.15 % in comparison to glucose stressed cells. About, 46.16 % ($P < 0.05$) and 35.35 % decrease in ROS generation was observed in pre-treated and post-treated hepatocytes (Fig. 2b). Naringenin did not cause cytotoxicity as no significant change in ROS generation was observed.

Expression of antioxidant genes and modulation in antioxidants enzymatic activities

To study the involvement of oxidative stress generated during high glucose stress, transcript levels of antioxidant genes like MnSOD, CuZn-SOD, GPx, and GR was studied by RT-PCR. Manganese superoxide dismutase is known to reduce mitochondrial ROS generation and Cyt-c release and hence is also considered an anti-apoptotic gene [34]. Hepatocytes cultured with high glucose showed decreased (1.49-fold, $P < 0.05$) level of MnSOD. The effect of hyperglycemia was abrogated by administration of

Table 2 Antioxidant status under varying concentrations of glucose in primary rat hepatocytes

Treatment	SOD activity (units/min/10 ⁴ cells)	Catalase activity (mM H ₂ O ₂ decomposed/min/10 ⁴ cells)	GSH content (μM/10 ⁴ cells)
Control	0.82 ± 0.01	7.81 ± 0.09	170.86 ± 8.59
Mannitol	0.83 ± 0.01	7.17 ± 0.05	160.90 ± 4.59
10 mM glucose	0.63 ± 0.01	7.86 ± 0.65	135.88 ± 2.78
20 mM glucose	0.64 ± 0.01	6.31 ± 0.57	111.18 ± 2.29
30 mM glucose	0.57 ± 0.05*	4.33 ± 0.96*	114.72 ± 1.07
35 mM glucose	0.56 ± 0.01*	2.46 ± 1.12*	80.74 ± 3.49*
40 mM glucose	0.27 ± 0.01*	2.21 ± 0.81*	65.62 ± 9.78*

Results are shown as mean ± SE from three independent experiments

* Significant difference compared with control values; $P < 0.05$, $n = 6$

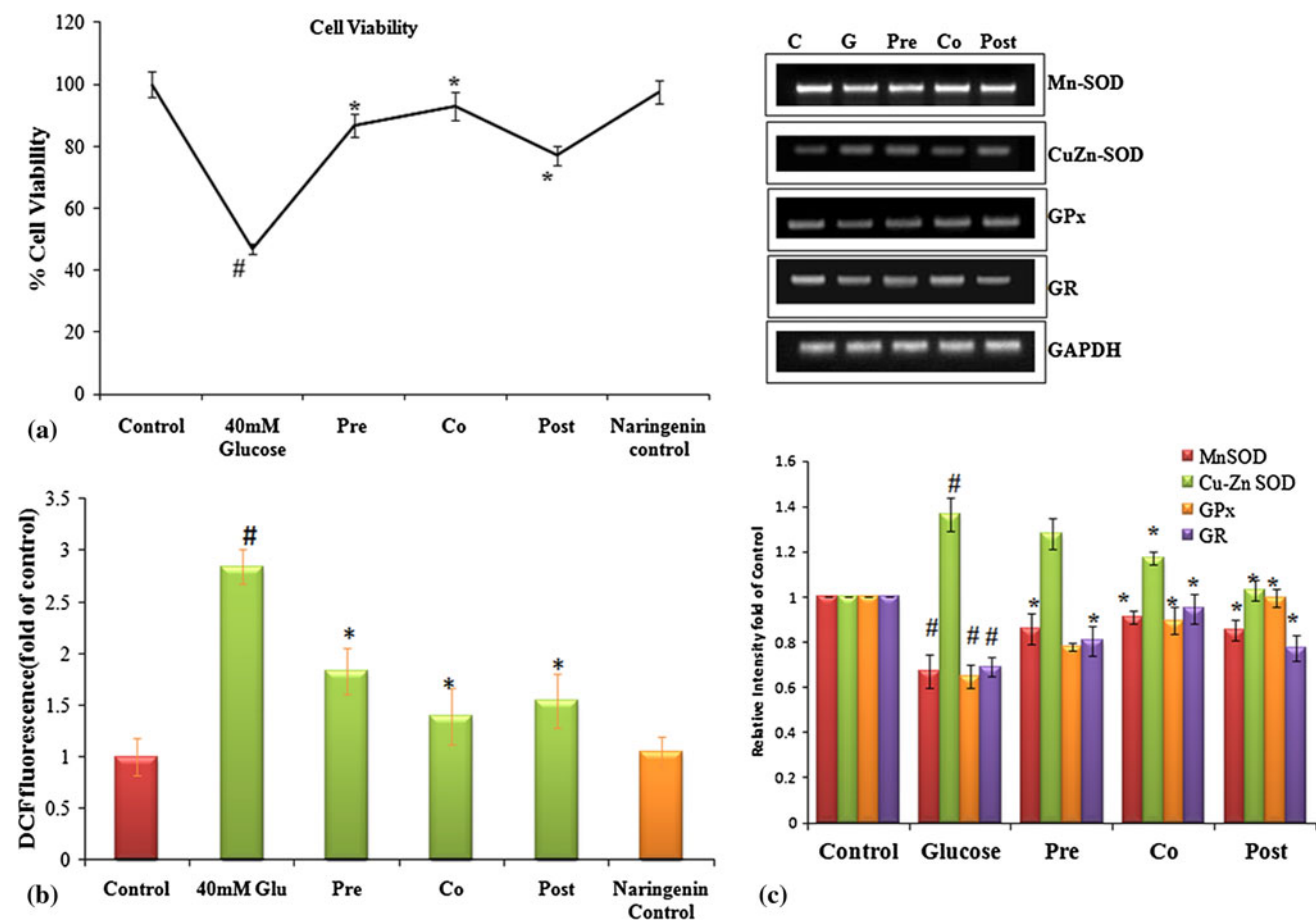


Fig. 2 Attenuation of cell viability, antioxidant gene expression and ROS stress by naringenin. Effect of naringenin on glucose-induced cytotoxicity in hepatocytes. **a** Cell viability in control, high glucose-treated (40 mM) and naringenin-treated cells. Relative viability is shown as the percentage of viable cells as compared to control, **b** ROS generation and **c** transcript levels of antioxidant genes. mRNA of MnSOD, Cu Zn-SOD, GPx and GR were amplified by RT-PCR,

GAPDH was used as internal control (Fig. 2c). Graphs show fold change in expression. Results are shown as mean ± S.E. # $P < 0.05$ denotes significant difference compared with control values. * $P < 0.05$ denote significant difference compared with 40 mM glucose-treated cells. Results are representative of three separate experiments. The SD was below ±5 % in all cases

naringenin. 1.58-fold ($P < 0.05$) restoration was observed in the level of MnSOD, in cells co-treated with naringenin. Level of CuZn-SOD was found to enhance by 1.36-fold in 40 mM glucose-treated hepatocytes, which decreased by 1.16-fold in cells pre-treated with naringenin. In stressed cells, CuZn-SOD possibly increased as a defence

mechanism to overcome the persistent oxidative stress. Expression of other antioxidant genes like GPx and GR was significantly reduced by 1.56- and 1.44-fold, respectively, on treatment with high glucose. Naringenin, on account of its antioxidant capacity, was able to decrease ROS generation and restored the level of antioxidant

Table 3 Modulation by naringenin in antioxidant status under high glucose stress in primary rat hepatocytes

Treatment	SOD activity (units/min/ 10^4 cells)	Catalase activity ($\mu\text{M H}_2\text{O}_2$ decomposed/min/ 10^4 cells)	GPx activity ($\mu\text{M NADPH}$ decomposed/min/ 10^4 cells)
Control	0.94 ± 0.01	8.01 ± 0.10	172.10 ± 5.129
Glucose	$0.32 \pm 0.05^\#$	$3.99 \pm 0.08^\#$	$98.12 \pm 3.76^\#$
Pre	$0.68 \pm 0.03^*$	$6.97 \pm 0.32^*$	$143.58 \pm 2.93^*$
Co	$0.79 \pm 0.01^*$	$7.154 \pm 0.8^*$	$163.39 \pm 24.86^*$
Post	$0.57 \pm 0.05^*$	$5.19 \pm 0.60^*$	$122.21 \pm 3.24^*$

Results are shown as mean \pm S.E. from three independent experiments

$^\#$ Significant difference compared with control values; * Significant difference compared with glucose treatment values; $^\#P < 0.05$, $^*P < 0.05$, $n = 6$

genes—GPx and GR to values comparable to control (Fig. 2c). High glucose significantly altered the enzymatic activity of hepatocytes. Activities of SOD, catalase, and glutathione peroxidase were significantly decreased ($P < 0.05$) in hepatocytes treated with high glucose, which were again significantly increased on pre, co and post treatment of naringenin. Naringenin in its co-treatment maximally modulated the enzymatic activities of SOD, catalase, and glutathione peroxidase ($P < 0.05$) (Table 3).

Effect of naringenin on mitochondrial membrane potential ($\Psi\Delta m$) in cells under glucose stress

Apoptosis begins when a cell activates its own destruction by initiating a series of complex cascading events that include depolarization of the mitochondria. Ability of glucose to alter the mitochondrial trans-membrane electrical potential was investigated in primary hepatocytes. As mitochondria get depolarized, the fluorescence of the JC-1 dye changes from red to green. An increase of monomeric JC-1 molecules (green fluorescence) due to a decrease of mitochondrial membrane potential occurred in glucose-stressed hepatocytes. 2.03-fold ($P < 0.05$) decrease in the ratio of red to green fluorescence occurred in glucose-stressed hepatocytes as the mitochondria became progressively depolarized. Treatment of cells with naringenin resulted in significant enhancement in red/green fluorescence with maximum increase of 2.54-folds observed in naringenin co-treated cells (Fig. 3a) indicating prevention of depolarization of mitochondria.

Expression of Bax and Bcl-2

To further clarify the scheme of events in hyperglycemia-induced stress, we investigated the changes in apoptotic

genes like Bax, and anti-apoptotic gene Bcl-2 at the transcript levels by RT-PCR and also translation level of Bax and Bcl-2. It was observed that expression of Bcl-2 significantly ($P < 0.05$) decreased by 1.44-fold in 40 mM glucose-treated cells. This decline in mRNA level of Bcl-2 was significantly prevented ($P < 0.05$) in cells co-treated and pre-treated with naringenin. Similar to PCR results, significant change of 2.12-fold in translational level of Bcl-2 was observed. Transcription and translation of pro-apoptotic gene-Bax was significantly ($P < 0.05$) enhanced in glucose-treated cells (1.92-fold). On treatment with naringenin it was significantly ($P < 0.05$) reduced by 2.42 fold (Fig. 3b).

Translocation of proteins

Release of mitochondrial proteins like cytochrome c, Endo-G, and AIF marks the major event during apoptosis. To analyze the translocation of Cyt-c, its protein level was quantified by western blot in mitochondrial and cytosolic fractions of control and treated hepatocytes. The level of cytochrome c was depleted from its resident location i.e. mitochondria, after treatment of primary hepatocytes with high concentration of glucose and increased in cytosolic fraction. The altered level of cytochrome c was restored on treatment with naringenin (Fig. 4a). Mitochondria are also reported to contain death effectors like Endo-G which during apoptosis translocates to nucleus where it causes oligo-nucleosomal DNA fragmentation. Hepatocytes when incubated with high concentration of glucose, showed marked increase in the levels of Endo-G in nuclear fraction (Fig. 4b).

Similarly, in hepatocytes incubated with high glucose there was twofold decrease in the level of AIF in mitochondria and a substantial increase (2.46-fold) in nuclear fraction. On treatment with naringenin, during all three exposure conditions- pre, co and post, the level of AIF was found to be enhanced in mitochondrial fraction and decreased in nuclear fraction indicating prevention of its translocation (Fig. 5b). Immuno-chemical detection also confirmed our observation that AIF was mainly found in the cytoplasmic region in control cells. However, the immuno-reactivity of AIF was clearly evident in the nuclei of cells exposed to high glucose stress conditions (Fig. 5a), corroborating the results obtained by western blotting. First panel depicts the nuclei, stained by Hoechst 33258, second panel depicts mitochondrion stained by mitotracker orange. Third panel shows AIF immuno-labelling indicating mitochondrial or nuclear localisation of AIF. In control cells, AIF is localized in mitochondria dispersed throughout cytoplasm. No AIF fluorescent labelling is seen inside the nuclei of control cells. Upon high glucose exposure, AIF was no longer co-localized with Mito-tracker. The overlaid picture clearly exhibited the presence of AIF in

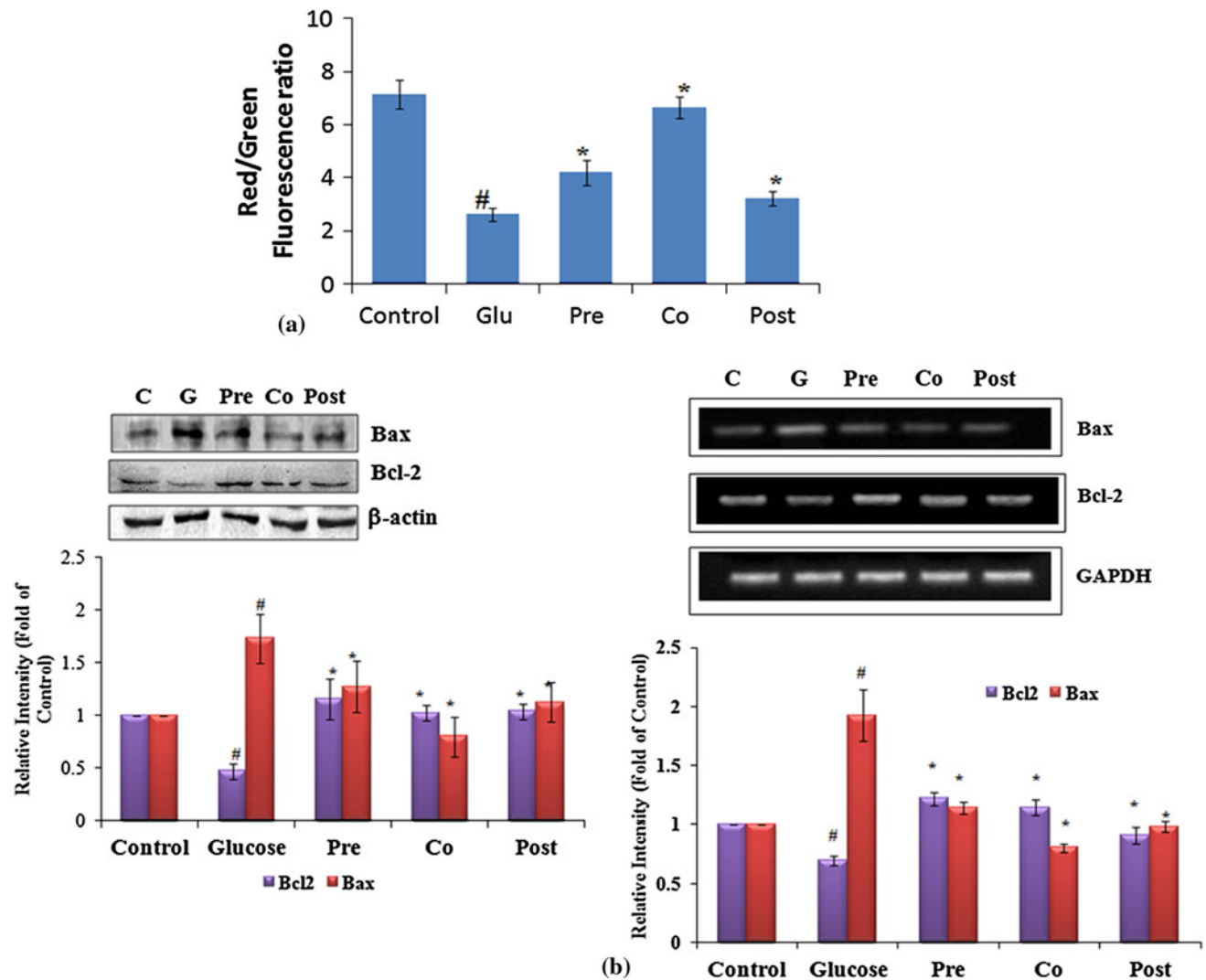


Fig. 3 Effect of naringenin on mitochondrial membrane potential (MMP), transcriptional and translational level of Bax and Bcl-2. Mitochondrial membrane potential in control, high glucose-treated (40 mM) and naringenin-treated cells is shown in (a). Decrease in the red/green fluorescence ratio reflects increased number of depolarized mitochondria. *Left panel* of (b) shows protein level of Bax and Bcl-2 as

estimated through western blot, β -actin served as loading control while *right panel* of (b) shows m-RNA level of Bcl-2 and Bax, using GAPDH as internal control. Densitometry shows relative intensity normalized to internal control. Results are shown as mean \pm SE. [#] $P < 0.05$ denotes significant difference compared with control values and ^{*} $P < 0.05$ denotes significant difference compared with 40 mM glucose

nucleus as stained by Hoechst 33258. On the whole, the results do indicate the presence of AIF translocation from the mitochondria to the nucleus in cells exposed to high glucose, suggesting that AIF release was involved in response to high glucose toxicity. In case of cells co-treated with naringenin, prevention of migration of AIF to nucleus is evident from distinct unlabeled nuclear space.

Expression of caspase-3/9 and caspase-3 enzymatic activity

Initiator and effector caspases along with Bax and Bcl-2 play a regulatory role in oxidative stress-induced

apoptosis. High glucose-treated hepatocytes exhibited increased expression of caspase-9 (initiator) and caspase-3 (effector) i.e. 1.44- and 1.99-fold ($P < 0.05$), respectively. Expression of caspase-9 and caspase-3 was decreased in naringenin-treated cells by 1.27- and 1.58-fold, respectively (Fig. 6a). Significant enhancement ($P < 0.05$) by 1.73- and 1.91-fold was observed in cleaved product of initiator and executioner caspase. Enzymatic activity of caspase-3 was significantly ($P < 0.05$) increased in high glucose-stressed hepatocytes. (Fig. 6b) Naringenin modulated the activity and a significant reduction of 2.5-folds ($P < 0.05$) was observed on co-treatment with naringenin (Fig. 6c).

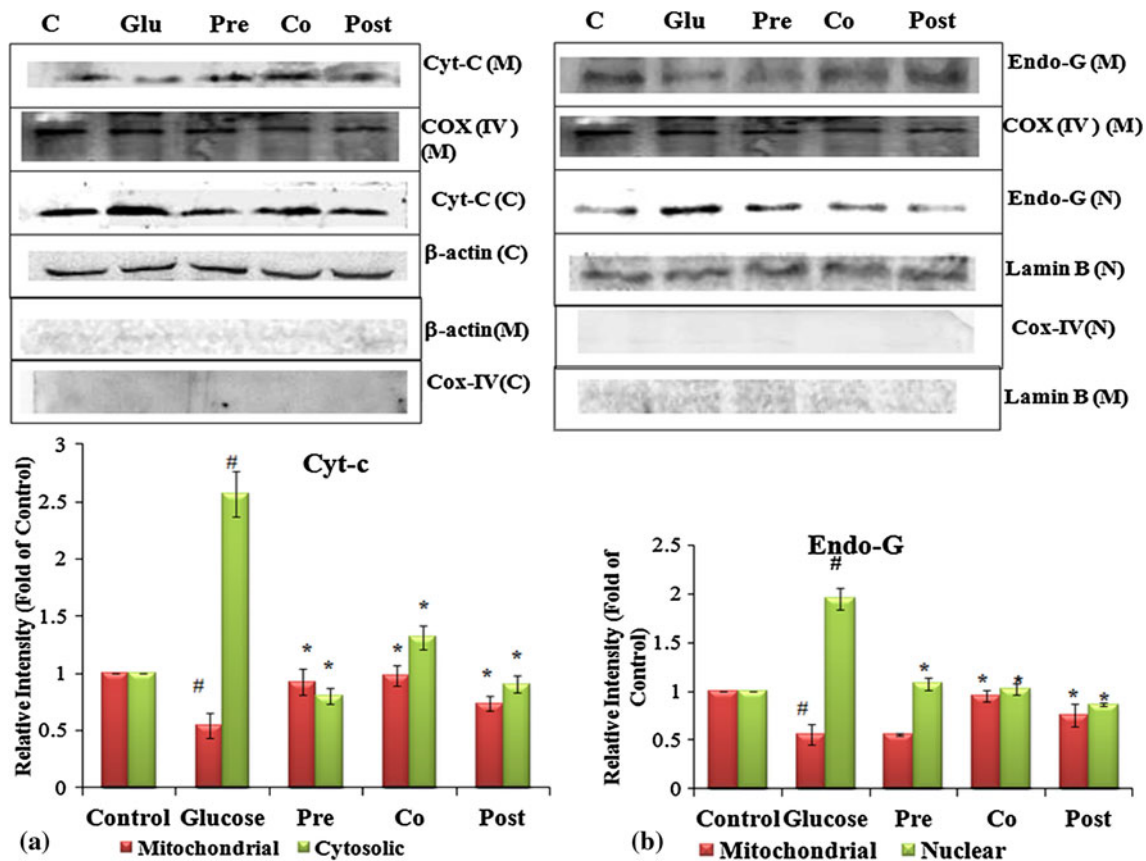


Fig. 4 Translocation of Cyt-c and Endo-G from mitochondria to nucleus. Glucose-induced cell death involves Cyt-c and Endo-G release from mitochondria. The changes in immunoreactivity for Cyt-c in the mitochondrial and cytosolic fractions were assessed. Mitochondrial Cyt-c was depleted significantly after high glucose treatment. Cox (IV) served as internal control for mitochondria (a). Cytosolic Cyt-c increased concomitantly upon high glucose treatment. β -actin served as internal control. **b** Endo-G release from mitochondria due to permeability changes and its translocation to nucleus. Changes in the immuno-reactivity for Endo-G, in the

mitochondrial and nuclear fractions were assessed. Mitochondrial Endo-G was depleted significantly after high glucose treatment while nuclear Endo-G increased concomitantly. Cox (IV) served as internal control for mitochondria and Lamin-B served as internal control for nuclear fraction. Densitometry shows relative intensity normalized to internal control. Results are shown as mean \pm SE. # $P < 0.05$ denotes significant difference compared with control values and * $P < 0.05$ denotes significant difference compared with 40 mM glucose. Results are representative of three separate experiments

Detection of apoptosis

DNA fragmentation Apoptosis is characterized by cytoplasmic condensation, plasma membrane blebbing, and nuclear pycnosis, leading to oligonucleosomal DNA breakdown. To examine apoptosis in the hepatocytes under high glucose condition, inter-nucleosomal DNA fragmentation (DNA-“laddering”) was assessed using electrophoresis. DNA samples from the control hepatocytes and hepatocytes pre and co-treated with naringenin showed no distinct bands, but high molecular weight mass was retained on the top portion of the gel (Fig. 7a, lane 2, 4 & 5). In contrast, a number of low molecular weight bands showing specific laddering pattern were observed in DNA samples obtained from the hepatocytes treated with high glucose indicating apoptosis.

Chromatin condensation Hoechst 33258 was used to study chromatin condensation, an important hallmark of apoptosis. Cells exposed to high glucose stress showed enhanced fluorescent intensity which corresponds to nuclear condensation. Cells pre- and co-treated with naringenin were significantly more resistant than untreated cells to high glucose-induced apoptosis and hence showed no change in nuclear morphology (Fig. 7b) whereas post-treatment did not show much protection against nuclear condensation.

Externalization of phosphatidyl serine Apoptosis in glucose-stressed primary rat hepatocytes was assessed by annexin V-FITC binding assay. In intact cells, phosphatidylserine is restricted to the inner side of the plasma membrane. However, during early apoptosis before the loss

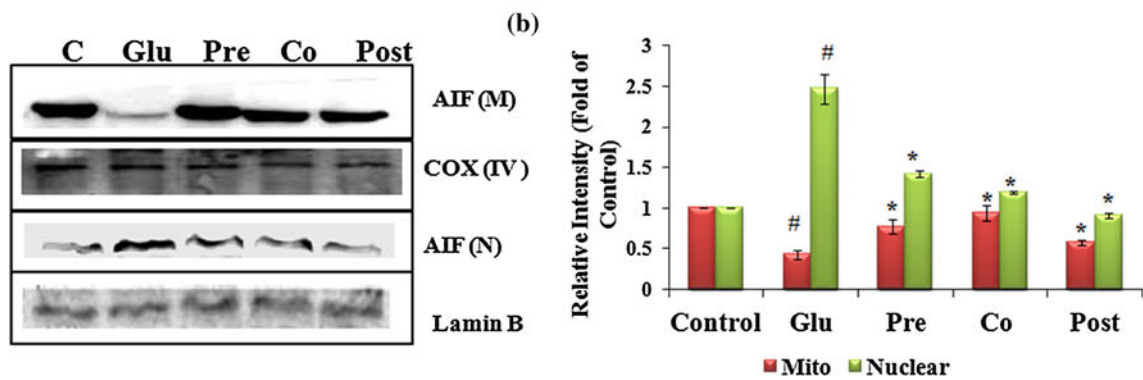
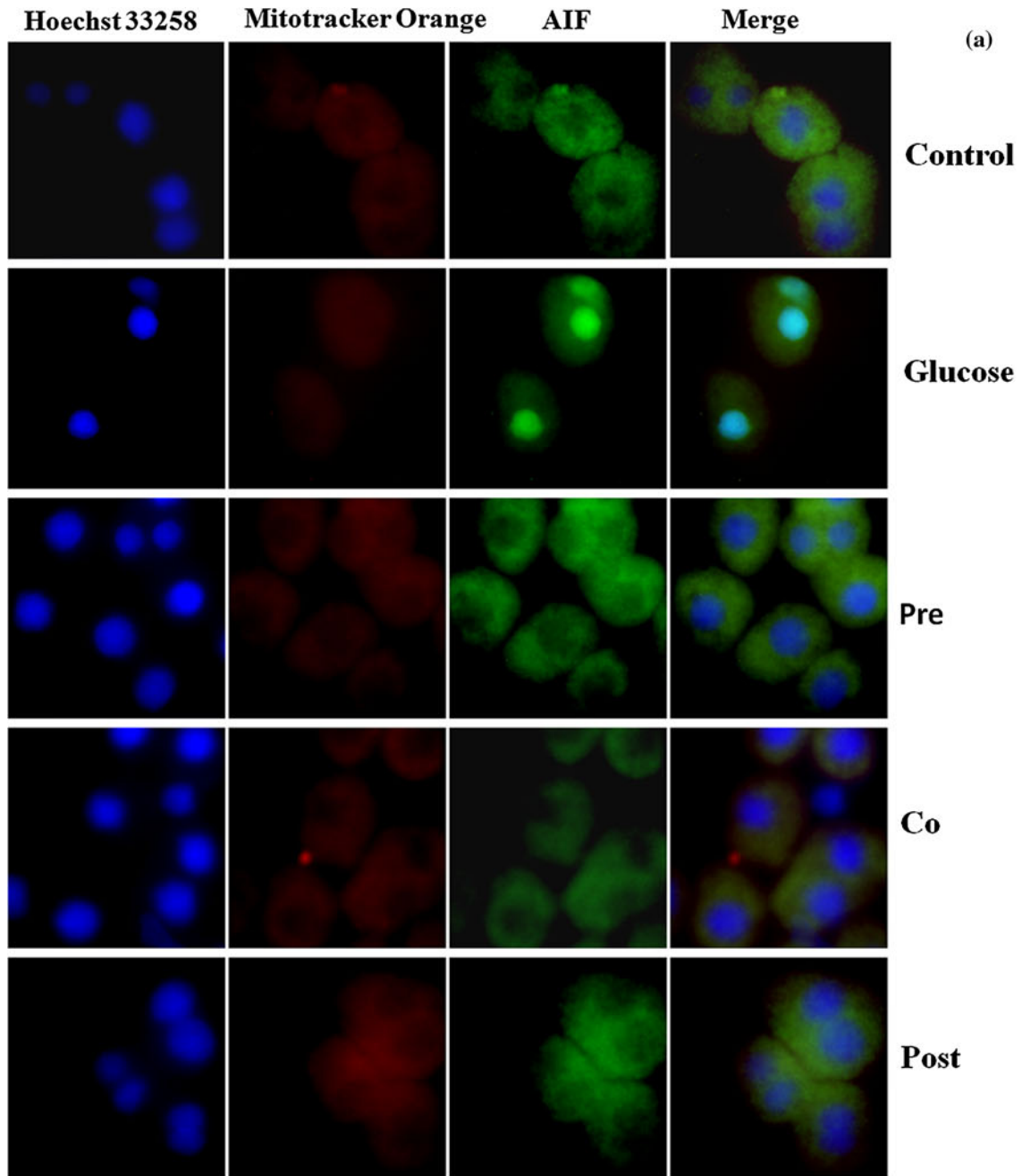


Fig. 5 Translocation of AIF from mitochondria to nucleus under glucose stress. Glucose-induced cell death involves AIF release from mitochondria. High glucose increased translocation of AIF from mitochondria to the nucleus. **a** Represents sub-cellular localization of AIF as analyzed by immunocytochemistry using FITC conjugated secondary antibody against AIF (green) and the nuclear marker Hoechst-33258 (blue), mitochondria stained by mitotracker orange (red). All the images were observed at $\times 63$ objective magnification. (For interpretation of the references in colour in this figure legend, the reader is referred to the web version of this article). Results are representative of three separate experiments. Figure 5b shows changes in the immunoreactivity of AIF in the mitochondrial and nuclear fractions with COX IV and Lamin-B serving as control for mitochondrial and nuclear fractions, respectively. $\#P < 0.05$ denotes significant difference compared with control values and $*P < 0.05$ denotes significant difference compared with 40 mM glucose (Color figure online)

of membrane integrity, phosphatidylserine appears on the outer side of the plasma membrane, marked by annexin V binding, followed by permeabilized membrane-stained with annexin V and PI and later compromised membrane marked by only PI stain. In control cells, 99.88 % of the cell population was found to be viable, 0.09 % cells were found to be in early apoptosis, and 0.03 % cells showed necrosis (Fig. 8a). In the cells treated with 40 mM glucose, 54.64 % were viable, 39.79 % in early apoptosis, 5.41 % in late apoptosis, whereas 0.16 % cells were undergoing necrosis. During co-treatment with naringenin, only 1.29 % cells were found to be in early apoptosis, 0.61 % in late apoptosis, 0.04 % cells underwent necrosis, and remaining 98.06 % cells were found to be viable. In

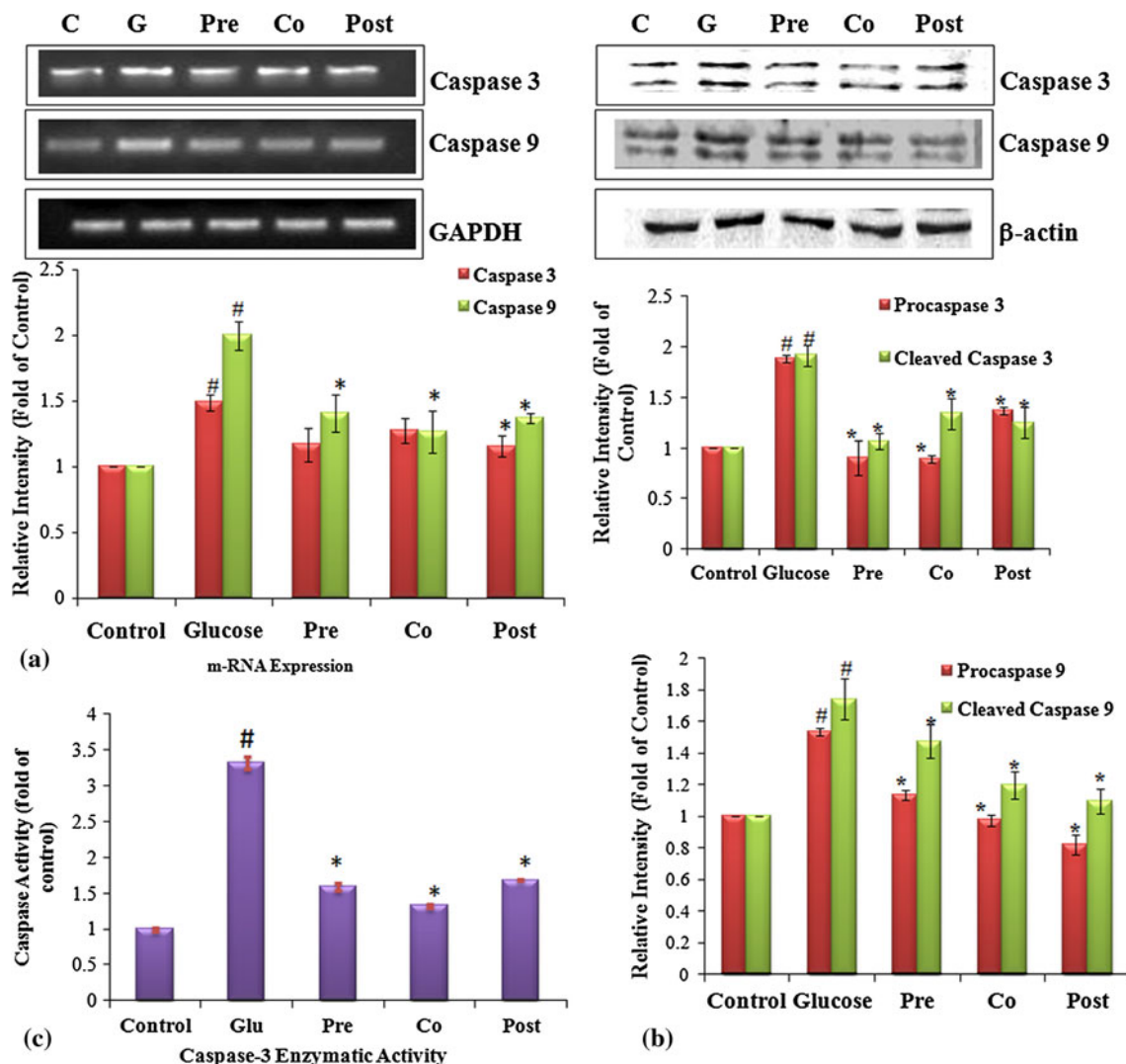


Fig. 6 Effect of naringenin on mRNA and protein levels of caspase-3/9 and enzymatic activity of caspase-3 **a** Shows mRNA level of apoptotic genes—caspase-3 and caspase-9 using GAPDH as internal control. Densitometry shows relative intensity normalized to internal control, **b** activation of caspase-3 and caspase-9 as evident from appearance of its cleaved product. Densitometry shows relative

intensity normalized to internal control. *Graph* of (c) caspase-3 enzymatic activity of control and stressed cells. Results are shown as mean \pm SE. $\#P < 0.05$ denotes significant difference compared with control values and $*P < 0.05$ denotes significant difference compared with 40 mM glucose-treated cells

pre-treatment with naringenin, 6.04 % cells were found to be in early apoptosis and 93.22 % cells were found to be viable. Similar results were obtained during post-treatment of cells.

Cell cycle analysis with cellular DNA content Cell cycle analysis with cellular DNA content was performed by flow cytometry. Apoptotic cells were estimated by calculating the number of sub-diploid cells in the cell cycle histogram. When cells were exposed to glucose, apoptotic cells increased markedly. The number of sub-diploid cells after glucose treatment was found to be 15.34 %. The percentage of sub-diploid cells in control population was only 1.45 %. Cells pre- and co-treated with naringenin decreased the apoptotic DNA content to 9.39 and 3.22 % respectively. Post-treatment did not cause much significant effect, however, the apoptotic DNA content was reduced to 10.43 % (Fig. 8b).

Discussion

The harmful effects of hyperglycemia play an important role in pathophysiology of diabetes. High glucose causes complications like nephropathy, cardiopathy, neuropathy, and many more affecting virtually all organs of the body [35, 36]. Oxidative stress has been shown to play a key role

Fig. 8 Naringenin modulates hyperglycemia-induced apoptotic changes observed during Annexin–PI staining and Apoptotic DNA content. Effect of naringenin on hyperglycemia-induced apoptosis in hepatocytes using Annexin–PI staining in control, high glucose-treated (40 mM) and naringenin-treated (pre, co and post-treated) stressed hepatocytes (Fig. 8a). The cells were stained with FITC–Annexin and PI, and analyzed on flowcytometer (Beckton Dickinson–LSR). The S.D. was below ± 5 % in all cases. Figure 8b shows effect of naringenin on hyperglycemia-induced changes in cell cycle. Control, high glucose-treated (40 mM) and naringenin-treated (pre, co and post-treated) stressed cells were stained with propidium iodide. Results are expressed as the % of sub-G1 population. SD was below ± 5 % in all the cases. Results are representative of three separate experiments

in high glucose-induced cell death [13, 37]. Prevention of generation of free radicals could constitute a major advancement in the treatment of diabetic complications. Since type 2 diabetes is characterized by extracellular glucose levels, the present study adds to the reported understanding of the mechanism by which chronic hyperglycemia influences cell function [38]. The aim of the study was to investigate molecular mechanism of glucose stress-induced apoptosis in primary rat hepatocytes and its amelioration by natural phyto-constituent naringenin.

Indirectly or directly, liver is the primary and major target organ of insulin action and glucose metabolism. Diabetes is followed by development of major biochemical and functional abnormalities in liver including alterations in carbohydrate, lipid, protein metabolism, and changes in

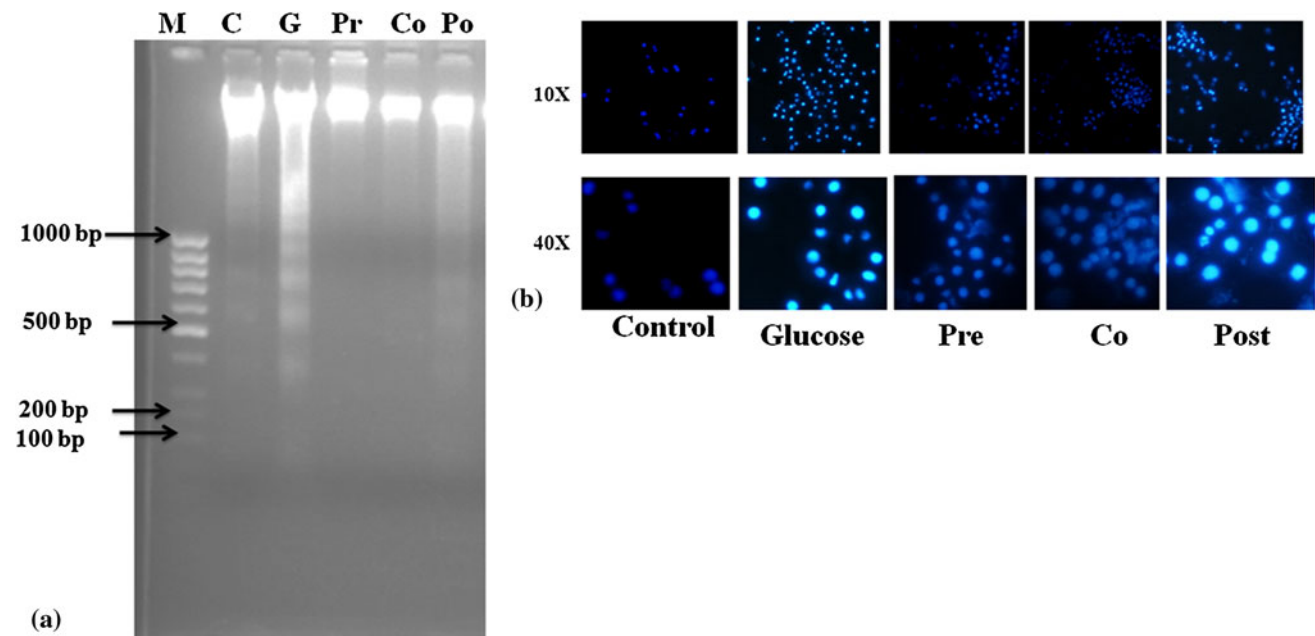


Fig. 7 Modulation of hyperglycemia-induced DNA fragmentation and chromatin condensation by naringenin. Intra-nucleosomal DNA fragmentation in control, high glucose-treated (40 mM) and naringenin-treated (pre, co and post-treated) stressed cells is shown in (a). Lane 1 DNA Marker 100 bp, Lane 2 Control DNA, Lane 3 DNA from 40 mM glucose-treated hepatocytes, Lane 4 naringenin pre-treatment,

Lane 5 naringenin co-treatment, Lane 6 naringenin post treatment. Results are representative of three separate experiments and **b** chromatin condensation. Rat hepatocytes were stained with Hoechst 33258 and visualized at $\times 10$ and $\times 40$ magnifications. Results are representative of three separate experiments

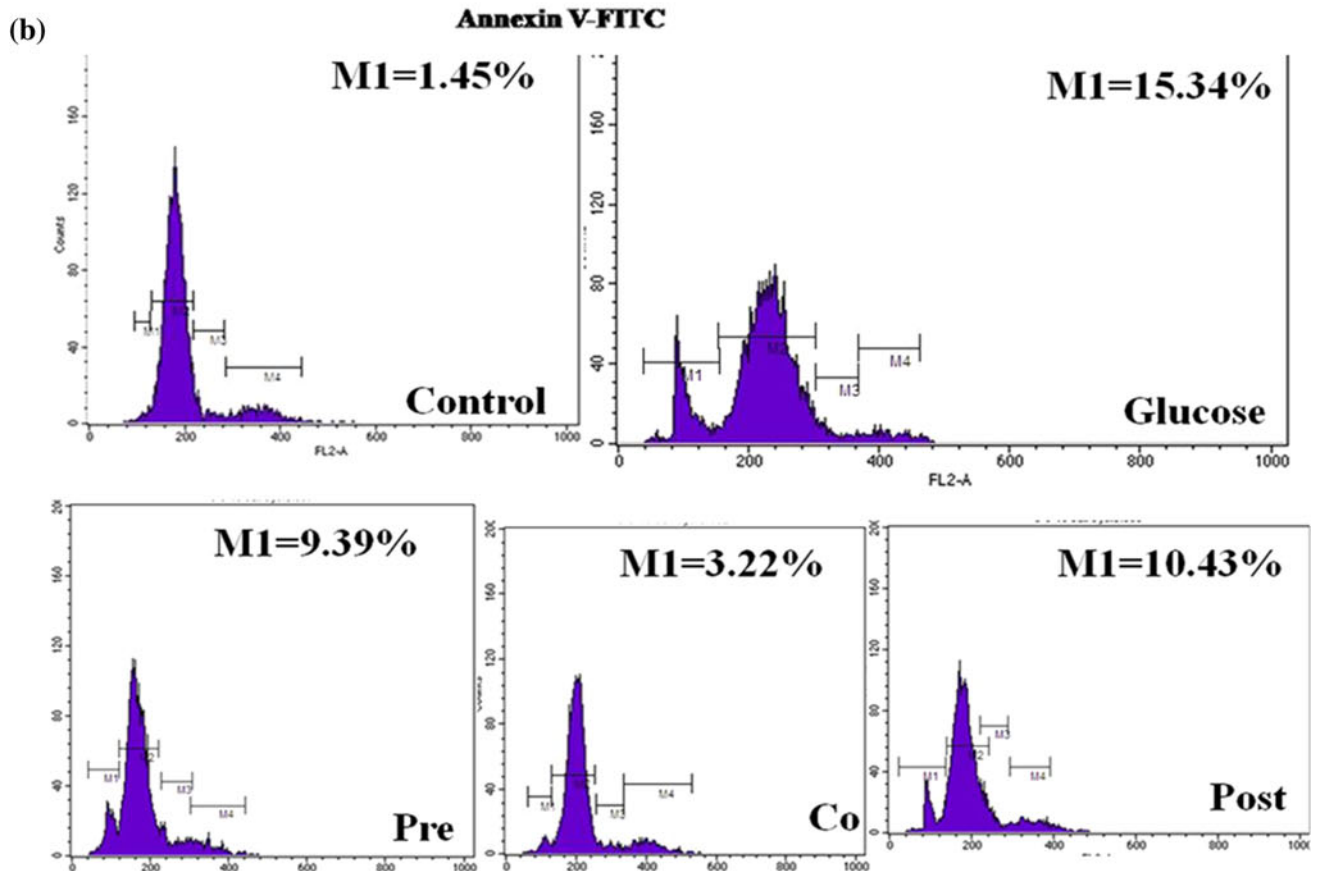
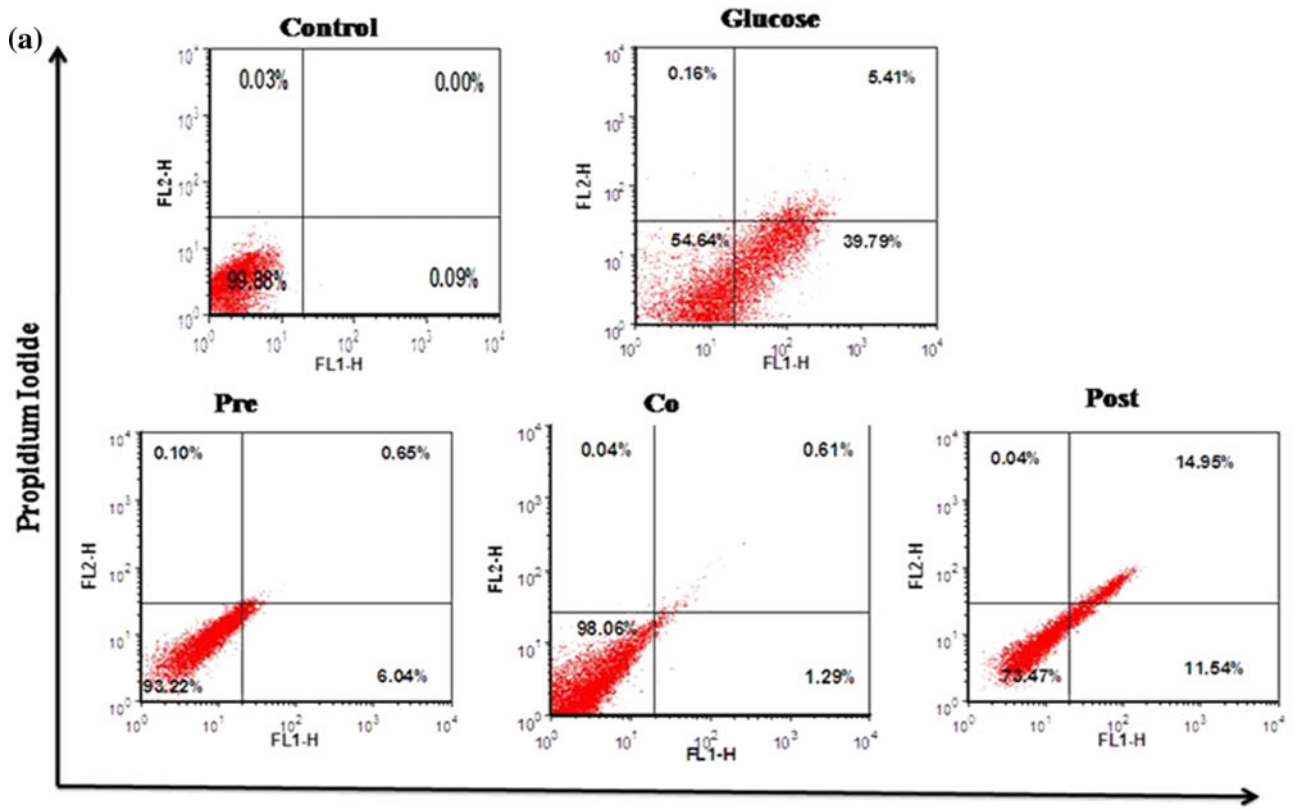
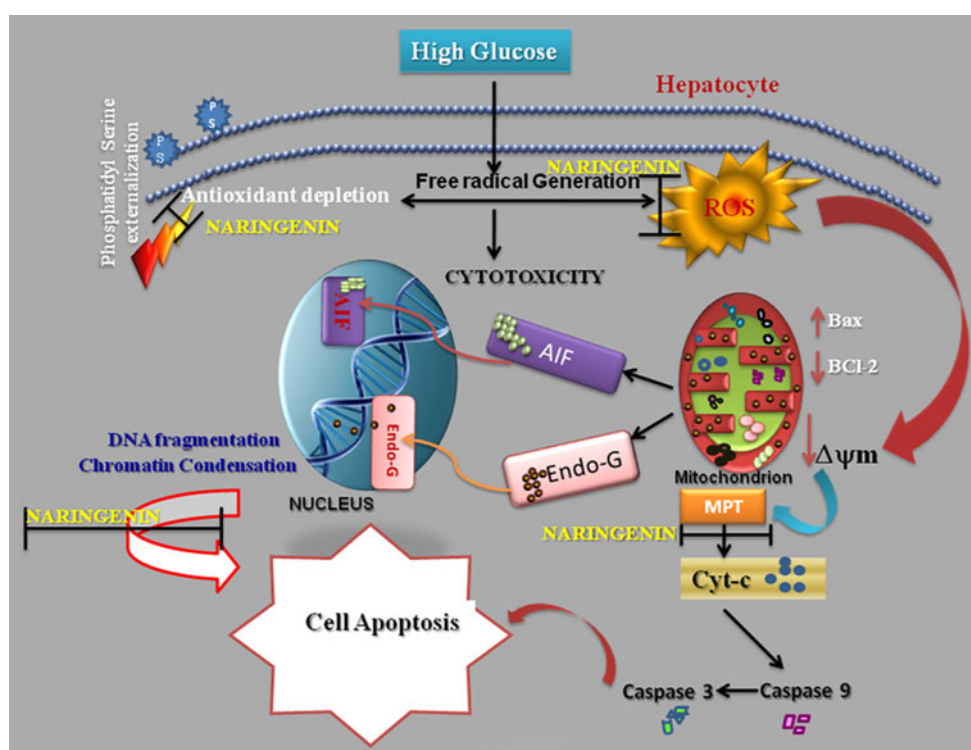


Fig. 9 Proposed mechanism of high glucose-induced hepatotoxicity. Several metabolic pathways lead to high glucose-induced ROS generation and alterations in antioxidant defenses. Continuous generation of ROS induces mitochondrial depolarization and permeability transition, resulting in release of apoptotic proteins from their resident place i.e. mitochondria to nucleus or cytosol. Apoptosis inducing factor and Endo-G are released from mitochondria and translocated to nucleus while Cyt-c translocates to cytosol. Further, with the activation of caspases, AIF and Endo-G trigger further signals for DNA fragmentation and chromatin condensation. Naringenin in this study, not only quenched free radicals, prevented ROS generation but also modulated the major hallmarks of oxidative stress induced apoptosis



antioxidant status [13]. Chronic hyperglycemia alters normal cellular environment of liver by affecting glucose, lipid, and bile dysregulation, triglyceride metabolism and several other cellular processes. High concentration of glucose in cells has been considered as model of hyperglycemia as effects produced at this concentration closely resemble diabetic ketoacidosis in vivo [9–11].

In the present study, hepatocytes cultured in RPMI-1640 replicate normal glycaemic condition of humans, whereas hepatocytes exposed to high concentration of glucose depicted hyperglycaemic condition. The relative concentration used in this study is consistent with other models of hyperglycemia and chronic human diabetes [18–20]. High glucose (40 mM) caused cytotoxicity, ROS generation and alterations in antioxidant status. On the contrary, no such deleterious effects were seen in hepatocytes exposed to similar concentration of mannitol, ruling out the possibility of involvement of hyper-osmolarity [8–10].

Generation of ROS under high glucose stress condition has been established in many cell types [2, 3] and our observations are consistent with the hypothesis that ROS plays a pivotal role in high glucose-induced apoptosis and free radical scavengers can block or delay this process [13]. The phytochemicals having antioxidant activity are known to abrogate the oxidative stress. Naringenin is known to have good antioxidant activity and hence authors investigated the capacity of naringenin to ameliorate high glucose-induced oxidative stress. The study reveals the

involvement of various antioxidant genes under high glucose stress. Messenger RNA level of various antioxidant genes like CuSOD, MnSOD, GPx, and GR was altered under high glucose stress which is in accordance with earlier reports suggesting modulated expression of antioxidant genes during high glucose-induced oxidative stress [5, 39]. In addition to change in transcript levels of antioxidant genes, significant alteration in the enzymatic activities was also seen. Naringenin ameliorated the ROS generation and prevented decline in antioxidant status during high glucose-induced stress. Diabetes is associated with disturbed antioxidant status. Naringenin being a good antioxidant and derived from anti-diabetic plant, can be put to effective use in diabetic patients.

Mitochondrial dysfunction is an important hallmark of programmed cell death (apoptosis). The role of mitochondria in the execution of apoptosis is crucial since this organelle is involved in the release of pre-apoptotic factors. Opening of MPT pore increases the mitochondrial membrane permeability resulting in release of apoptogenic proteins like Cyt-c, AIF, Endo-G, and collapse of $\Psi\Delta m$ leading to subsequent cell death. Decrease in mitochondrial membrane potential has been reported by many researchers in different cell types [38–40]. Our result of decreased mitochondrial membrane potential in high glucose-treated hepatocytes is in accordance to the earlier reports of mitochondrial dysfunction as a result of high glucose in different cell types [41, 42]. Naringenin, on one hand

reduces ROS, on the other hand also augments the mitochondrial membrane potential affecting the release of various apoptogenic factors from mitochondria. While preventing mitochondrial depolarization, naringenin caused decline in the release of apoptogenic factors from mitochondria and increased expression of anti-apoptogenic factors like Bcl-2.

Translocation of AIF from mitochondria to nucleus is a major checkpoint of apoptosis and also influences DNA damage. In this study, AIF translocated from mitochondria to nucleus where it induced chromatin condensation and DNA damage. The increase in apoptosis and DNA damage correlates well with translocation of AIF and Endo-G from mitochondria to nucleus. Increase in AIF content in nucleus under high glucose stress was further confirmed by immunocytochemical studies. We also found that caspase-3 and caspase-9 were up-regulated in addition to AIF and Endo-G translocation to nucleus. The changes in mitochondrial membrane potential, release of cytochrome c, Endo-G, and AIF together with activation of caspase-9 and -3, indicates a prominent role of mitochondria in high glucose-induced cell death.

The alterations induced by high glucose in nuclear morphological features of primary hepatocytes completely reflect the classic apoptotic morphological features of chromatin condensation, chromatin marginalization to the nuclear envelope, and nuclear fragmentation to form apoptotic bodies. On treating high glucose-stressed hepatocytes with naringenin, apoptotic population, DNA fragmentation, and chromatin condensation were significantly decreased. This was further confirmed by externalization of phosphatidyl serine as evident from double staining of hepatocytes with Annexin V–PI and apoptotic DNA content as evident from PI staining. High glucose-treated hepatocytes exhibited remarkable increase in Annexin V–PI binding and peak of sub G1 population. On treating high glucose-stressed hepatocytes with naringenin, apoptotic population, DNA fragmentation, and chromatin condensation were significantly decreased. Among the three treatments of naringenin, co-treatment was found to be most effective in ameliorating mitochondria-mediated apoptosis caused by high glucose stress in primary hepatocytes. The post-treatment of cells has shown some protective effect, although to a lesser extent than co-treatment. This is indicative of its therapeutic potential. However, in vivo experiments designed to study post-treatment effect can provide confirmation regarding its therapeutic benefits. Since naringenin was effective against hyperglycemia in all the three treatment schedules, findings of the present study suggest that naringenin can be effectively used as prophylactic as well as therapeutic agent against diabetes which is associated with

altered antioxidant status, mitochondrial depolarization, and apoptosis.

Conclusion

The current findings propose a chronological sequence of events related to the effects of high glucose on primary hepatocytes. Analyses of expression of Bcl-2 family genes and proteins, antioxidant genes, and their activities, generation of ROS, the sub-cellular locations of cytochrome c, AIF, Endo G, and activation of caspase-9/3 suggest that apoptosis induced by high glucose in primary rat hepatocytes is primarily associated with promotion of ROS production, mitochondrial dysfunction, and DNA damage (Fig. 9). Naringenin, a flavonoid, significantly improved antioxidant status and inhibited the critical control points of apoptotic pathway studied. Although several mechanisms may interplay in the protective effect of naringenin, the present results indicate that antioxidant effects of naringenin along with its capacity to alter critical control points of apoptosis may be responsible for its anti-apoptotic capacity against high glucose toxicity in primary hepatocytes and hence may exert beneficial effects in preventing diabetes-associated complications in liver.

Acknowledgments Authors express their deep gratitude to Dr. K. C. Gupta, Director IITR for his kind support to this work. Authors are grateful to Indian Council of Medical Research, New-Delhi for fellowship and Supra-institutional project (SIP-08) for financial support. Authors also thank the IITR publication review committee for allocating the manuscript number 2947.

Conflict of interest None.

References

1. World Health Organization; Media Centre, Diabetes, Facts and Figures, Fact sheet N312 August 2011. <http://www.who.int/mediacentre/factsheets/fs312/en/index.html>
2. Sato Y, Feng GG, Huang L, Fan JH, Chang An J, Koji T, Kurokawa S, Fujiwara Y, Toru K, Kondo F, Ishikawa N (2010) Enhanced expression of naofen in kidney of streptozotocin induced diabetic rats: possible correlation to apoptosis of tubular epithelial cells. *Clin Exp Nephrol* 14:205–212. doi:10.1007/s10157-010-0276-1
3. Mokini Z, Marcovecchio ML, Chiarelli F (2010) Molecular pathology of oxidative stress in diabetic angiopathy: role of mitochondrial and cellular pathways. *Diabetes Res Clin Pract* 87:313–321. doi:10.1016/j.diabres.2009.11.018
4. Choi SW, Benzie IFF, Ma SW, Strain JJ, Hannigan BM (2008) Acute hyperglycemia and oxidative stress: direct cause and effect? *Free Radic Biol Med* 44:1217–1231. doi:10.1016/j.freeradbiomed.2007.12.005
5. Cusi K (2009) Nonalcoholic fatty liver disease in type 2 diabetes mellitus. *Curr Opin Endocrinol Diabetes Obes* 16:141–149. doi:10.1097/med.0b013e3283293015

6. Dey A, Swaminathan K (2010) Hyperglycemia-induced mitochondrial alterations in liver. *Life Sci* 87:197–214. doi:[10.1016/j.lfs.2010.06.007](https://doi.org/10.1016/j.lfs.2010.06.007)
7. Kakkar P, Singh BK (2007) Mitochondria: a hub of redox activities and cellular distress control. *Mol Cell Biochem* 305:235–253. doi:[10.1007/s11010-007-9520-8](https://doi.org/10.1007/s11010-007-9520-8)
8. Palmeira CM, Rolo AP, Berthiaume J, Bjork JA, Wallace KB (2007) Hyperglycemia decreases mitochondrial function: the regulatory role of mitochondrial biogenesis. *Toxicol Appl Pharmacol* 225:214–220. doi:[10.1016/j.taap.2007.07.015](https://doi.org/10.1016/j.taap.2007.07.015)
9. Malfitano C, Tatiana C, Loureiro A, Rodrigues B, Sirvente R, Salemi VMC, Rabechi NB, Lacchini S, Curi R, Irigoyen MCC (2010) Hyperglycemia protects the heart after myocardial infarction: aspects of programmed cell survival and cell death. *Eur J Heart Fail* 12:659–667. doi:[10.1093/eurjhf/hfq053](https://doi.org/10.1093/eurjhf/hfq053)
10. Chandrasekaran K, Swaminathan K, Chatterjee S, Dey A (2010) Apoptosis in HepG2 cells exposed to high glucose. *Toxicol In Vitro* 24:387–396. doi:[10.1016/j.tiv.2009.10.020](https://doi.org/10.1016/j.tiv.2009.10.020)
11. Leal EC, Aveleira CA, Castilho AF, Serra AM, Baptista FI, Hosoya KI, Forrester JV, Ambrosio AF (2009) High glucose and oxidative/nitrosative stress conditions induce apoptosis in retinal endothelial cells by a caspase-independent pathway. *Exp Eye Res* 88:983–991. doi:[10.1016/j.exer.2008.12.010](https://doi.org/10.1016/j.exer.2008.12.010)
12. Chen Y, Lewis W, Diwan A, Cheng EHY, Matkovich SJ, Dorn GW (2010) Dual autonomous mitochondrial cell death pathways are activated by Nix/BNip3L and induce cardiomyopathy. *Proc Natl Acad Sci* 20:9035–9042. doi:[10.1073/pnas.0914013107](https://doi.org/10.1073/pnas.0914013107)
13. Frances DE, Ronco MT, Monti JA, Ingaramo PI, Pisani GB, Parody JP, Pellegrino JM, Sanz PM, Carrillo MC, Carnovale CE (2010) Hyperglycemia induces apoptosis in rat liver through the increase of hydroxyl radical: new insights into the insulin effect. *J Endocrinol* 205:187–200. doi:[10.1677/JOE-09-0462](https://doi.org/10.1677/JOE-09-0462)
14. Purushotam A, Tian M, Belury MA (2009) The citrus fruits flavanoids naringenin suppresses hepatic glucose production from Fao hepatoma cells. *Mol Nutr Food Res* 53:300–307. doi:[10.1002/mnfr.200700514](https://doi.org/10.1002/mnfr.200700514)
15. Sohn E, Kim J, Kim CS, Kim YS, Jang DS, Kim JS (2010) Extract of the aerial parts of *Aster koraiensis* reduced development of diabetic nephropathy via anti-apoptosis of podocytes in streptozotocin-induced diabetic rats. *Biochem Biophys Res Commun* 391:733–738. doi:[10.1016/j.bbrc.2009.11.129](https://doi.org/10.1016/j.bbrc.2009.11.129)
16. Rajadurai M, Stanelly P, Prince M (2007) Preventive effect of naringenin on isoproterenol-induced cardiotoxicity in Wistar rats: an in vivo and in vitro study. *Toxicology* 232:216. doi:[10.1016/j.tox.2007.01.006](https://doi.org/10.1016/j.tox.2007.01.006)
17. Seglen PO (1976) Preparation of isolated rat liver cells. *Methods Cell Biol* 19:187–191
18. Chu HL, Chien JC, Duh PD (2011) Protective effect of *Cordyceps militaris* against high glucose-induced oxidative stress in human umbilical vein endothelial cells. *Food Chem* 129:871–876. doi:[10.1016/j.foodchem.2011.05.037](https://doi.org/10.1016/j.foodchem.2011.05.037)
19. Leininger GM, Russell JW, van Golen CM, Berent A, Feldman EL (2004) Insulin-like growth factor-I regulates glucose-induced mitochondrial depolarization and apoptosis in human neuroblastoma. *Cell Death Differ* 11(8):885–896. doi:[10.1038/sj.cdd.4401429](https://doi.org/10.1038/sj.cdd.4401429)
20. Russell JW, Golovoy D, Vincent AM, Mahendru P, Olzmann JA, Mentzer A, Feldman EL (2002) High glucose-induced oxidative stress and mitochondrial dysfunction in neurons. *FASEB J* 16(13):1738–1748. doi:[10.1096/fj.01-1027](https://doi.org/10.1096/fj.01-1027)
21. Varma S, Lal BK, Zheng R, Breslin JW, Saito S, Pappas PJ, Hobson RW II, Durán WN (2005) Hyperglycemia alters PI3K and Akt. *Am J Physiol Heart Circ Physiol* 289(4):H1744–1751. doi:[10.1152](https://doi.org/10.1152)
22. Hornick T, Aron D (2008) Preventing and managing diabetic complications in elderly patients. *Cleaveland Clin J Med* 75:153–158. doi:[10.3949/ccjm.75.2.153](https://doi.org/10.3949/ccjm.75.2.153)
23. Cloherty JP, Eichenwald EC, Hansen AR, Stark AR (2012) *Manual of Neonatal Care*. Lippincott Williams & Wilkins
24. Mosmann T (1983) Rapid colorimetric assay for cellular growth and survival: application to proliferation and cytotoxicity assays. *J Immunol Methods* 65:55–63. doi:[10.1016/0022-1759\(83\)90303-4](https://doi.org/10.1016/0022-1759(83)90303-4)
25. Kakkar P, Vishwanathan PND (1984) A modified spectrophotometric assay of superoxide dismutase. *Indian J Biochem Biophys* 21:130–132
26. Aebi H (1984) Catalase In vitro. *Methods Enzymol* 113:121–126
27. Dringen R, Hamprecht B (1996) Glutathione content as an indicator for the presence of metabolic pathways of amino acids in astroglial cultures. *J Neurochem* 67:1375–1382. doi:[10.1046/j.1471-4159.1996.67041375.x](https://doi.org/10.1046/j.1471-4159.1996.67041375.x)
28. Paglia DE, Valentine WN (1967) Studies on qualitative and quantitative characterization of erythrocytes Glutathione Peroxidase. *J Lab Clin Med* 70:158–169
29. Zhang J, Liu Y, Yang HW, Xu HY, Meng Y (2008) Molecular mechanism of beta cell apoptosis induced by p58 in high glucose medium. *Arch Pharm Res* 31:357–363
30. Tripathi M, Singh BK, Mishra C, Raisuddin S, Kakkar P (2010) Involvement of mitochondria-mediated pathways in hepatoprotection conferred by *Fumaria parviflora Lam.* extract against nimesulide-induced apoptosis in vitro. *Toxicol in Vitro* 24:495–508. doi:[10.1016/j.tiv.2009.09.011](https://doi.org/10.1016/j.tiv.2009.09.011)
31. Lowry OH, Rosebrough NJ, Farr AL, Randall RJ (1951) Protein measurement with the Folin-phenol reagent. *J Biol Chem* 193:265–275
32. Rodrigues CMP, Sola S, Nani Z, Castro RE, Ribeiro PS, Walter C, Low C, Steer CJ (2003) Tauroursodeoxycholic acid reduces apoptosis and protects against neurological injury after acute hemorrhagic stroke in rats. *Proc Natl Acad Sci* 100:6087–6092. doi:[10.1073/pnas.1031632100](https://doi.org/10.1073/pnas.1031632100)
33. Nigam N, George J, Srivastava S, Roy P, Bhui K, Singh M, Shukla Y (2010) Induction of apoptosis by [6]-gingerol associated with the modulation of p53 and involvement of mitochondrial signaling pathway in B[a]P-induced mouse skin tumorigenesis. *Cancer Chemother Pharmacol* 65:687–696. doi:[10.1007/s00280-009-1074-x](https://doi.org/10.1007/s00280-009-1074-x)
34. Thureau M, Marquardt G, Laurent NG, Weinlander K, Naschberger E, Jochmann R, Alkharsah KR, Schulz TF, Thome M, Neipel F, Sturzl M (2009) Viral inhibitor of apoptosis vFLIP/K13 protects endothelial cells against superoxide-induced cell death. *J Virol* 83:598–611. doi:[10.1128/jvi.00629-08](https://doi.org/10.1128/jvi.00629-08)
35. Kapoor R, Srivastava S, Kakkar P (2009) Bacopa monnieri modulates antioxidant responses in brain and kidney of diabetic rats. *Environ Toxicol Pharmacol* 27:62–69. doi:[10.1016/j.etap.2008.08.007](https://doi.org/10.1016/j.etap.2008.08.007)
36. Pang J, Gong H, Xi C, Fan W, Dai Y, Zhang TM (2011) Poly (ADP-ribose) polymerase 1 is involved in glucose toxicity through SIRT1 modulation in HepG2 hepatocytes. *China J Cell Biochem* 112:299–306
37. Meng L, Cui L (2008) Inhibitory effects of crocetin on high glucose-induced apoptosis in cultured human umbilical vein endothelial cells and its mechanism. *Arch Pharm Res* 31:357–363. doi:[10.1007/s12272-001-1164-y](https://doi.org/10.1007/s12272-001-1164-y)
38. Sutovsky MP, Latham KE, Han Z, Vassena R, Chi MMY, Potireddy S, Sutovsky M, Kelle H (2008) Role of glucose in cloned mouse embryo development. *Am J Physiol Endocrinol Metab* 295:798–809. doi:[10.1152/ajpendo.00683.2007](https://doi.org/10.1152/ajpendo.00683.2007)
39. Bell DS, Allbright E (2007) The multifaceted associations of hepatobiliary disease and diabetes. *Endocr Pract* 13:300–312
40. Velagapudi C, Bhandari BS, Simone S, Abboud HE, Habib SL (2011) The Tuberin/mTOR pathway promotes apoptosis of tubular epithelial cells in diabetes. *J Am Soc Nephrol* 22:262–273. doi:[10.1681/asn.2010040352](https://doi.org/10.1681/asn.2010040352)

41. Mustapha NM, Tarr JM, Kohner EM, Chibber R (2010) NADPH oxidase versus mitochondria-derived ROS in glucose-induced apoptosis of pericytes in early Diabetic retinopathy. *J Ophthalmol*. doi:[10.1155/2010/746978](https://doi.org/10.1155/2010/746978)
42. Fei AL, Roy S (2009) High glucose-induced downregulation of connexin 43 expression promotes apoptosis in microvascular endothelial cells. *Invest Ophthalmol Vis Sci* 50:1400–1407. doi:[10.1167/iovs.07-1519](https://doi.org/10.1167/iovs.07-1519)